Encapsulation, Permeability, and Cellular Uptake Characteristics of Hollow Nanometer-Sized Conductive Polymer Capsules†

ARTICLE *in* THE JOURNAL OF PHYSICAL CHEMISTRY B · AUGUST 2001

Impact Factor: 3.3 · DOI: 10.1021/jp010820d

5 AUTHORS, INCLUDING:

Stella Marinakos
Duke University
28 PUBLICATIONS **1,871** CITATIONS
SEE PROFILE

Joseph Anthony Ryan
Iona College
6 PUBLICATIONS **1,360** CITATIONS
SEE PROFILE

Encapsulation, Permeability, and Cellular Uptake Characteristics of Hollow Nanometer-Sized Conductive Polymer Capsules†

Stella M. Marinakos,‡ Miles F. Anderson,‡ Joseph A. Ryan,‡ Linda D. Martin,§ and Daniel L. Feldheim*,‡

Departments of Chemistry and Anatomy, Physiological Sciences and Radiology, North Carolina State University, Raleigh, North Carolina 27695

Received: March 5, 2001; In Final Form: June 16, 2001

The use of nanometer-sized gold particles as templates for the synthesis of hollow poly(pyrrole), poly(*N*-methylpyrrole), and poly(3-methylthiophene) is described in this paper. Diffusion coefficients of small molecules through the capsule shell were found to vary by almost 3 orders of magnitude depending on the polymer, polymer oxidation state, and counteranion incorporated during polymer synthesis. A small molecule (anthraquinone) and an enzyme (horseradish peroxidase) were trapped inside hollow capsules by attaching them to the template particle prior to polymerization and particle etching. A thin poly(pyrrole) shell protected the enzyme 2 times longer in neat toluene compared to unencapsulated enzyme. Finally, the potential for using conductive polymer nanoparticles for intracellular delivery or diagnostics was examined by administering partice suspensions to 3T3 murine fibroblasts. Particles ranging in size from 25 to 100 nm were engulfed by fibroblasts without compromising cell viability.

Introduction

Nanoscale materials design and synthesis is important in the fabrication of advanced devices for optics, electronics, and biotechnology.[1] In biotechnology, the encapsulation and delivery of proteins and DNA into cells has led to the implementation of intracellular medicinal therapies such as gene therapy.[2] Future success in gene therapy will depend largely on the formulation of a deeper understanding of the genetic origins of disease, and on the ability to deliver large quantities of a chosen therapeutic agent into a cell without adversely affecting normal cellular processes. Completion of the human genome project has ensured the former, leaving the synthesis of encapsulation and delivery materials as perhaps the single most important challenge in intracellular medicinal therapies.

In previous work, our group described new methods for synthesizing nanometer-sized hollow capsules of poly(pyrrole), poly(*N*-methylpyrrole), and polyalkenes.[3] These methods utilized nanometer-sized gold particles as templates from which to grow polymer shells. Dissolution of the template particles yielded structurally intact hollow polymer capsules with interior volume and shell thickness governed by the diameter of the template particle and the polymerization time, respectively. Moreover, we showed that (i) alkanethiols were encapsulated in the hollow polymer core by attaching them to the gold template particles prior to polymerization and particle etching and (ii) small molecule diffusion rates through the pyrrole-based polymer capsules depended on polymer oxidation state.

Here we show that small molecules and enzymes can be trapped inside poly(pyrrole), poly(*N*-methylpyrrole), and poly(3-methylthiophene) capsules synthesized using the gold particle template method. We have also extended our diffusion studies to include polymers synthesized using a range of charge-balancing anions. Apparent diffusion coefficients in these capsules varied by about 2 orders of magnitude. In addition, the ability of a polymer shell to prevent enzymatic denaturation in organic solvents was tested. We found that the enzyme horseradish peroxidase (HRP) maintained its activity approximately 2 times longer in an organic solvent when encapsulated by even a thin poly(pyrrole) shell. Finally, cellular uptake and compatibility were addressed by feeding poly(pyrrole) capsules to a 3T3 fibroblast cell line and monitoring cell viability. Poly(pyrrole) capsules were engulfed by fibroblasts with little effect on cell viability.

Experimental Section

All reagents (monomers, electrolytes, organic solvents) were purchased from Aldrich and used as received. Horseradish peroxidase was purchased from Pierce. Gold particles were either purchased from Ted Pella or, for particles capped with anthraquinone (vide infra), synthesized using procedures described by Brust and co-workers.[1h] 3T3 murine fibroblast cells were purchased from ATCC (Rockville, MD). Dulbecco's Modified Eagle's Medium (DMEM) was purchased from BioWhittaker. All other cell culture materials and reagents (PBS, trypsin, DMSO, L-glutamine, fetal bovine serum, antibiotics, well plates, coverslips) were purchased from Fisher. Trypan blue viability assay was acquired from Sigma. Lactate dehydrogenase (LDH) colorimetric toxicity assay (CytoTox. 96) was purchased from Promega. A Leica laser scanning confocal microscope (reflection and transmission mode) was utilized to characterize particle uptake.

Anthraquinone-terminated hexanethiol was synthesized following a modified method of Zhang and co-workers.[4] To a solution of 0.8 g of NaH (60% oil dispersion, 20 mmol) in 100 mL of degassed THF, 1.21 g of 1-chloroanthraquinone (5 mmol) and 1.5 g of 1,6-hexanedithiol (10 mmol) were added. The solution was stirred for 3 h at room temperature and then poured

† Part of the special issue "Royce W. Murray Festschrift".

* Address correspondence to Dan_Feldheim@NCSU.edu.
‡ Department of Chemistry.
§ Department of Anatomy, Physiological Sciences and Radiology.

10.1021/jp010820d CCC: $20.00
Published on Web 08/04/2001

into 200 mL of ice water and acidfied to pH 5 with 1 M HCl. The solution was extracted with CH_2Cl_2 (4 × 50 mL), and the combined extractions were washed with H_2O (2 × 50 mL) before drying over $MgSO_4$. The solvent was evaporated and the yellow solid was washed with hexanes. The solid was then washed with 1:1 hexanes/CH_2Cl_2, and the orange wash solution was rotary evaporated to yield an orange solid. NMR revealed seven aromatic protons (7.5−8.5 ppm), six aliphatic protons (t 3.0 ppm, q 2.55 ppm, m 1.4−1.9 ppm), and one SH proton (t 1.33 ppm).

Synthesis of Hollow Polymer Nanocapsules. Poly(pyrrole) and poly(*N*-methylpyrrole) capsules were synthesized using the solid-support method described previously.[3a,b] Briefly, gold particles were loaded into the pores of an Al_2O_3 filtration membrane (Fisher Scientific, 0.02 μm diameter pores) by vacuum filtration. An aqueous solution of $[Fe(A)_3]$ initiator (A = ClO_4^-, NO_3^-, Cl^-) was placed above the membrane, and several drops of neat monomer were placed below the membrane.[3a,b] Monomer vapor quickly filled the membrane pores, polymerized, and precipitated onto the gold particles.

Poly(3-methylthiophene) capsules were synthesized using a variation of the template method described above. The gold particle loaded membrane was clamped in a U-tube, and acetonitrile solutions containing 3-methylthiophene (0.5 M) monomer and $[Fe(ClO_4)_3]$ (1.0 M) were placed on opposing sides of the membrane. Fe^{3+} and 3-methylthiophene diffused through solution into the membrane pores where poly(3-methylthiophene) formed around the gold particles.

The conductive polymer/gold particle composite nanostructures were converted to hollow polymer capsules by rinsing the membrane with gold etch solution (0.1 M KCN/0.001 M $K_3[Fe(CN_6)]$ to remove the template particle. The membrane was subsequently dissolved with 0.05 M KOH, and the capsules were isolated by alternately centrifuging and washing with aqueous solution three times.

Encapsulation. To illustrate small molecule encapsulation, anthraquinone (AQ) was covalently linked to gold nanoparticles via a hexanedithiol spacer. Poly(3-methylthiophene was polymerized around AQ−gold conjugates using $Fe(ClO_4)_3$ as described above.

Enzyme encapsulation was accomplished by combining 400 μg of HRP with a suspension of gold particles and stirring for 24 h. The HRP−gold particle conjugates were loaded into an Al_2O_3 membrane and rinsed thoroughly to remove any free HRP. Fe^{3+} could not be used as an initiator to encapsulate HRP because this strong oxidant deactivates the enzyme. However, it has been shown previously that HRP and H_2O_2 can initiate the oxidative polymerization of certain monomers.[5] Indeed, as shown below, we found that poly(pyrrole) formed using this method.

Enzyme activity was monitored with a standard TMB assay-(TMB is 3,5,3′,5′-tetramethylbenzidine; Pierce). The assay follows the reactions[6]

$$\text{HRP} + \text{H}_2\text{O}_2 \rightarrow \text{compound I} \quad (1)$$

$$\text{compound I} + \text{TMB} \rightarrow \text{compound II} + [\text{TMB}\bullet]^+ \quad (2)$$

$$\text{compound II} + \text{TMB} \rightarrow \text{HRP} + [\text{TMB}\bullet]^+ \quad (3)$$

where active HRP is indicated qualitatively by the appearance of the deep blue charge-transfer complex (λ_{max} = 370 nm, 652 nm) that forms between two $[TMB^\bullet]^+$ ions. To quantitate the number of active HRP enzymes encapsulated, a calibration curve was generated in which the amount of charge-transfer complex produced after 1 min was plotted vs HRP concentration. To stop the reaction as close to 1 min as possible, the assay solution was quenched with 2 M H_2SO_4. This converts the charge-transfer product to a two-electron oxidation diimine, with a stronger absorbance at 450 nm.

The calibration curve was exploited as follows. First, a known amount of gold particles was coated with HRP. The suspension of gold−HRP conjugates was then loaded into an Al_2O_3 membrane and rinsed with H_2O (3 × 50 mL). Visible spectroscopy of the filtrate revealed that an undetectable amount of gold passed through the membrane on the first H_2O rinse; free HRP was detected on the first rinse using the assay but not on subsequent rinses. However, some of the conjugate did adsorb to the face of the membrane. These were removed with a Kim wipe and subtracted out by comparing the gold absorbance at 520 nm prior to and following the wipe. The HRP−gold conjugates were encapsulated with poly(pyrrole) and assayed by placing the membrane in the assay solution. The solution contacting the membrane was stirred to ensure rapid transport of $[TMB^\bullet]^+$ out of the membrane. The assay was quenched after 1 min and examined by visible spectroscopy to determine the number of HRPs per gold particle. The rate of $[TMB^\bullet]^+$ diffusion through the thin poly(pyrrole) shell was not considered in the calculation. This source of error places a lower limit on the number of HRP enzymes per capsule.

Results and Discussion

Formation of Conductive Polymer/Gold Particle Composites. Representative transmission electron micrographs (TEM) of poly(pyrrole), poly(*N*-methylpyrrole), and poly(3-methylthiophene) shells coated onto gold particles are shown in Figure 1 along with corresponding plots of thickness vs time. Note that polymer shells ranging in thickness from 5 to 50 nm are obtained readily. The decrease in deposition rate at longer times is an expected consequence of radial growth. Considering geometry alone, as the surface area of the polymer increases with time, the increase in polymer thickness is expected to decrease.

Treating the composite materials shown in Figure 1 with gold etch solution resulted in structurally intact hollow capsules (Figure 2). The inner diameter of the capsules matched the diameter of the template particle, suggesting that little reorganization, collapse, or shrinkage occurs when the capsules are dried for TEM.

Guest Encapsulation. Encapsulation of AQ-terminated hexanethiol was followed by UV−visible spectroscopy. The absorbance at 460 nm in the spectrum in Figure 3 reveals that AQ is present after the polymer capsule forms, and following exposure to gold etch solution to remove the template particle. TEM confirmed that the gold particles were completely removed after exposure to the etch solution (not shown). Prolonged immersion of these capsules in CH_3CH_2OH solution resulted in no diminution of AQ absorbance, indicating that these molecules were trapped permanently inside the capsules.

Exposing HRP-coated gold nanoparticles to pyrrole and H_2O_2 resulted in poly(pyrrole) shells. However, in contrast to polymerization with Fe^{3+}, only relatively thin polymer skins (ca. 5 nm) were obtained even after long polymerization times (Figure 4). This is likely a consequence of diminished transport of H_2O_2 and growing oligomers as poly(pyrrole) surrounds the HRP initiator.

Enzyme encapsulation was characterized with a TMB assay. To determine the amount of enzyme lost during capsule

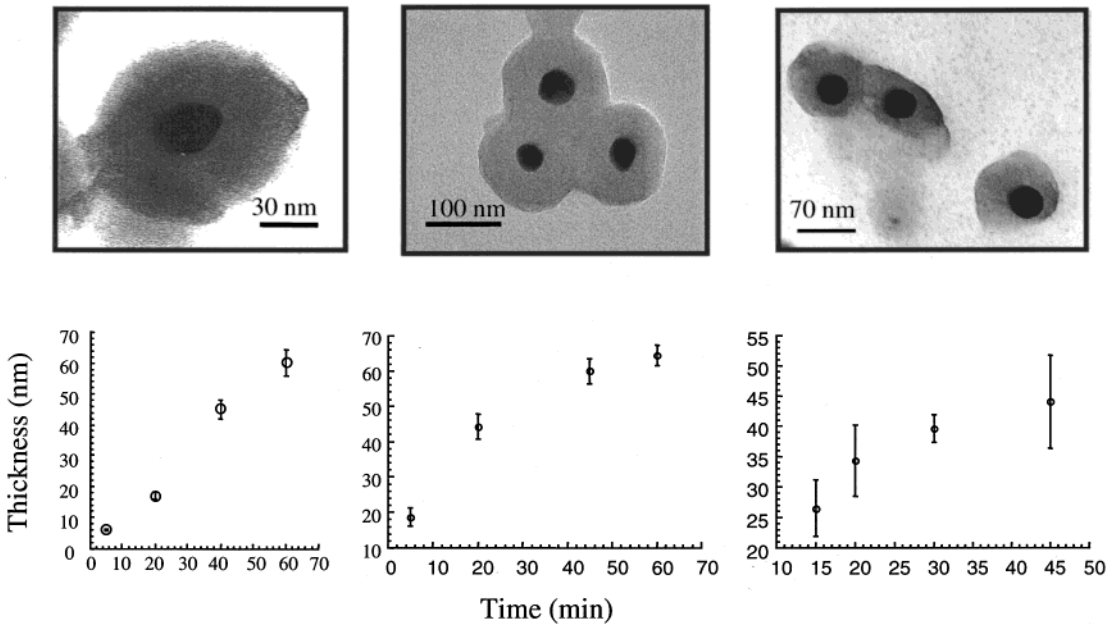

Figure 1. Transmission electron micrographs of (top left to right) poly(pyrrole)-, poly(*N*-methylpyrrole)-, and poly(3-methylthiophene)-coated gold particles. Bottom left to right shows corresponding plots of thickness vs polymerization time.

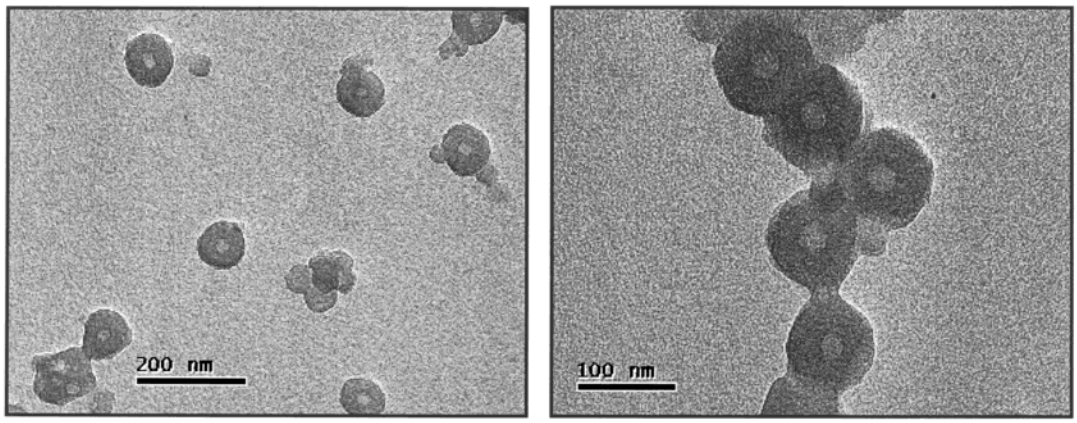

Figure 2. Transmission electron micrographs of hollow poly(*N*-methylpyrrole) (left) and poly(3-methylthiophene) (right) capsules.

formation via displacement or deactivation, the number of enzymes conjugated to 30 nm gold particles prior to and following encapsulation with poly(pyrrole) was determined. Prior to encapsulation there were an average of 2.8 active HRPs per particle (Table 1). This amount decreased to 1.4 and 0.9 following pyrrole polymerization and removal of the template particle, respectively. The decrease assumes that the only mechanisms for HRP loss are deactivation or displacement during capsule polymerization. Slower diffusion rates of H_2O_2 or TMB through the polymer shell would also contribute to the apparent decrease of active enzyme.

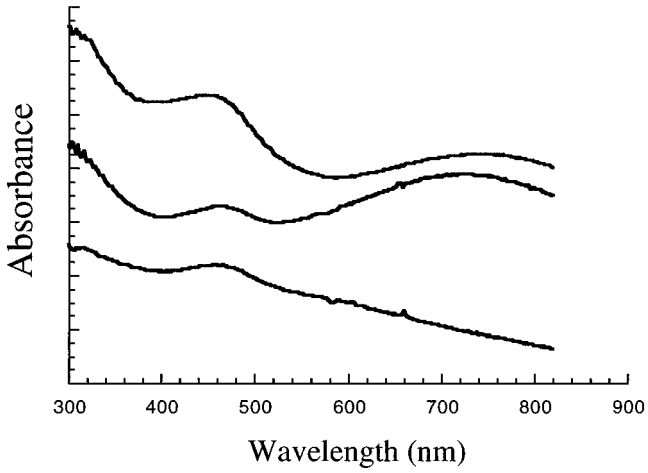

Figure 3. (bottom) UV−visible spectrum of anthraquinone-coated gold particles (diameter ca. 2 nm). (middle) Spectrum of anthraquinone-coated gold particles coated with poly(3-methylthiophene). (top) Spectrum acquired after treating particles with gold etch solution (see text for details). (Spectra offset for clarity.)

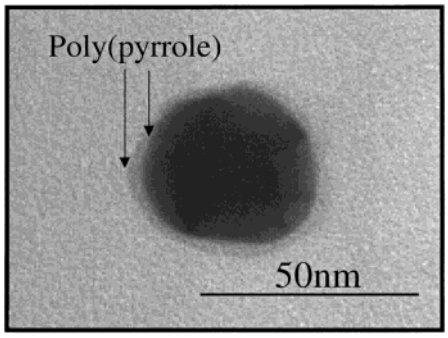

Figure 4. Transmission electron micrograph of poly(pyrrole) polymerized using horseradish peroxidase−gold particle conjugates as the initiator.

TABLE 1: Number of Active HRP Enzymes Loaded into Poly(pyrrole) Capsules

composite	active HRPs/particle	% loss of enzyme activity following 3 h in toluene	% loss of enzyme activity following 6 h in toluene
Au/HRP	2.8	90.2	97.4
Au/HRP/Ppy	1.4	39.8[a] (70.4)	72.1[a] (86.3)
HRP/Ppy	0.9		

[a] Percent loss of activity vs number of active HRPs on Au/HRP/Ppy. Number in parentheses is % vs Au/HRP.

As a crude measure of the porosity of the thin poly(pyrrole) shell, and to determine the extent to which a poly(pyrrole) capsule protects HRP from deactivating agents, the capsules were exposed separately to two different deactivating agents, aqueous Fe^{3+} and toluene. Our hypothesis was that cationic poly(pyrrole) could act as a hydrophilic, cation exclusion membrane, thus preventing cations and organic solvents from reaching the enzyme. Indeed, some protection was afforded against toluene. After 3 and 6 h in neat toluene, 60% and 28%, respectively, of the active encapsulated HRP remained active, compared to 10% and 3% for unencapsulated HRP. However, we observed that Fe^{3+} diffused quickly through the oxidized poly(pyrrole) capsule and degraded 100% of the HRP within 10 min.

In their current form poly(pyrrole) capsules do not provide sufficient protection to perform enzyme catalysis in harsh solvent environments. Better protection may be provided in the future by (i) synthesizing thicker polymer shells or (ii) slowing diffusion. To formulate a better understanding of the polymer structure−function relationships which might affect small molecule transport, we sought a quantitative measure of diffusion in conductive polymer capsules. These studies are reported below.

Diffusion through Conductive Polymer Capsules. An intriguing aspect of organic conductive polymer delivery systems is that small molecule diffusion rates through these materials depend on the redox state of the polymer. We previously showed that apparent diffusion coefficients for the etchant molecules diffusing into poly(pyrrole-ClO_4) capsules were approximately 2 orders of magnitude lower than for poly(*N*-methylpyrrole-ClO_4) and nearly 3 orders of magnitude lower than neutral poly(*N*-methylpyrrole).[3a]

Here we show that small molecule transport rates in conductive polymer capsules are also affected by the counterion present during poly(pyrrole) formation. Diffusion coefficients were measured for the etchant molecules diffusing through poly(*N*-methylpyrrole-A) films for the series A = ClO_4^-, NO_3^-, Cl^-. Etchant transport was measured spectroscopically by monitoring the disappearance of the gold particle plasmon extinction following the introduction of the etchant solution to an Al_2O_3 membrane loaded with polymer-coated gold particles. Absorbance vs time profiles were then fit to a model for diffusion in a spherical polymer (eq 4)[3a]

$$(\mathrm{abs}_t/\mathrm{abs}_0) = b\exp(-At); A = D\pi^2/L^2 \qquad (4)$$

where abs_0 and abs_t are the gold plasmon absorbances prior to etching and at time t during etching, respectively, and L is shell thickness. The term "apparent diffusion coefficient", D_{app}, is used because etchant diffusion into the sphere is likely hindered by transport of cyanoaurate complexes (e.g., $[Au(CN)_2]^+$, $[Au(CN)_4]^-$) out of the capsule interior. Thus, while the absolute

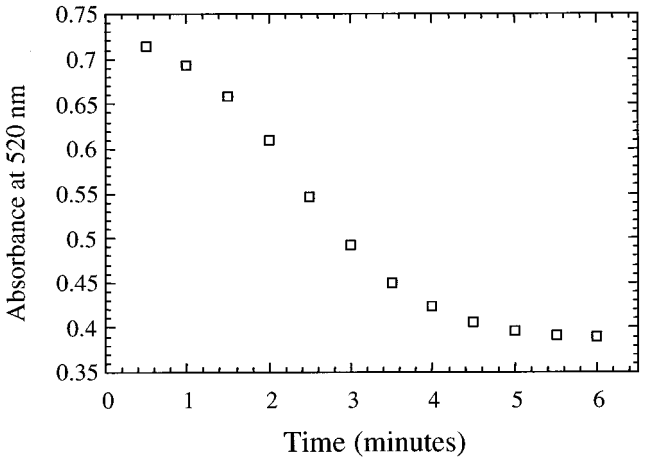

Figure 5. Gold nanoparticle absorbance vs etch time for poly(pyrrole-Cl).

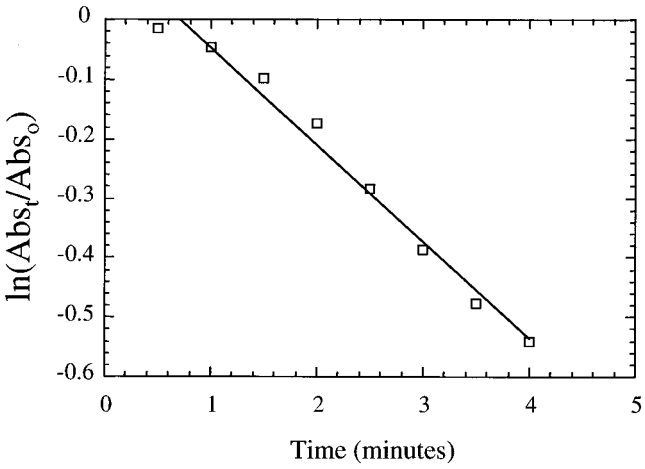

Figure 6. Fit of the data in Figure 5 to an equation for diffusion in a spherical polymer. The first data point was omitted from the fit to account for mixing. Since the absorbance remains constant after 4 min, the assumption was made that the particle was completely dissolved in this time. The last four data were thus also ommitted from the fit.

TABLE 2: Diffusion Coefficients for Poly(pyrrole) and Poly(*N*-methylpyrrole) Capsules

polymer	D (cm^2/s) × 10^{10}
PNMP	9.0
PNMP-ClO_4	3.0
Ppy-NO_3	4.4
Ppy-Cl	1.3
Ppy-ClO_4	0.34

D_{app} values reported below may be low, comparisons of relative transport rates are informative.

A representative plot showing the disappearance of the template particle vs time and a fit of these data to eq 4 for poly(pyrrole-A) capsules are shown in Figures 5 and 6, respectively. Although the data are not as well described by the diffusional model as the analogous data for poly(*N*-methylpyrrole)[3a], D_{app} values spanning an order of magnitude were estimated (Table 2). Differences in D_{app} between neutral and oxidized poly(*N*-methylpyrrole) capsules were rationalized previously by their densities, 1.0 g/cm^2 and 1.5 g/cm^2, respectively.[3a,7] The other trends in Table 2 are more difficult to justify. The difference between D_{app} in poly(*N*-methylpyrrole-ClO_4) and poly(pyrrole-ClO_4) shells suggests that the former is more porous. However, this finding contrasts previous measurements of porosity in these polymers by Martin et al.[8] Note also that there is no obvious trend in D_{app} vs anion. One might expect a trend based on anion

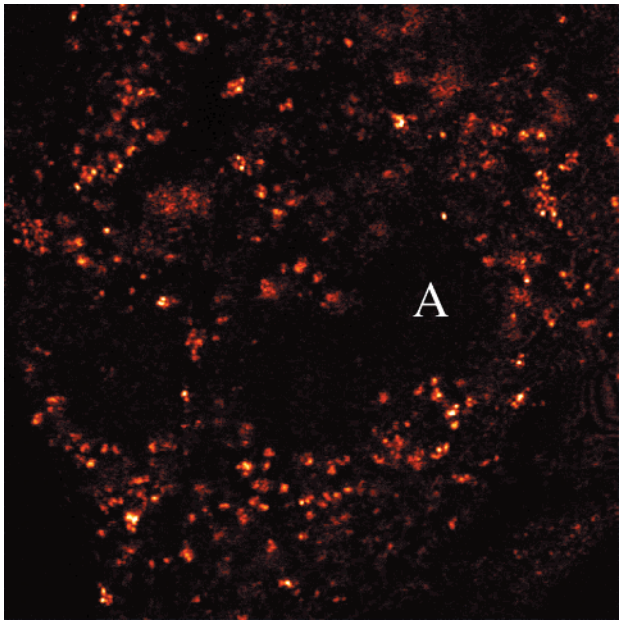

Figure 7. Confocal optical micrograph (reflection mode) of 3T3 murine fibroblasts containing poly(pyrrole) particles (bright spots in left image). The "A" marks a fibroblast nucleus where no particles were found.

TABLE 3: Results of the Trypan Blue Cell Toxicity Test

particle size (nm)	% viability
26	98.0
73	98.0
100	93.4
control	97.6

TABLE 4: Results of the LDH Cell Toxicity Test

particle size (nm)	% viability
26	83.8
73	83.6
100	83.6
control	83.1

size. However, while the largest anion studied, ClO_4^-, does give the smallest D_{app}, the smallest anion, Cl^-, does not yield the largest D_{app}. We suspect these deviations are a result of anion geometry and charge density which complicate the simple size arguments.

Cellular Uptake. Important issues to address when designing nanoscopic particles for intracellular delivery are (i) particle stability in growth media, (ii) mechanism of uptake, (iii) particle destination, (iv) particle size limitations on cellular uptake, and (v) cell viability following particle ingestion. These issues were addressed by suspending three different sizes of poly(pyrrole) capsules (ca. 25, 70, and 100 nm diameter) in DMEM culture medium. 3T3 fibroblast cells were grown to approximately 50% confluency on 1.5 mm coverslips in 12-well plates. Colloidal suspensions of poly(pyrrole) nanoparticles were administered, and the cells were further incubated at 37 °C and 10.1% CO_2 for 24 h. Confocal microscopy and TEM revealed that poly(pyrrole) capsules remained as stable suspensions in the growth medium and that particles were ingested by the fibroblasts (Figure 7). The particles were found engulfed in vesicles thoughout the cytoplasm, suggesting pinocytotic uptake. Biocompatibility of the capsules was investigated utilizing trypan blue and LDH colorimetric viability assays (corrected for polymer absorbance). Results of these biochemical assays are reported in Tables 3 and 4, respectively. Compared to control cells, these assays show that poly(pyrrole) capsules do not impart any deleterious effects to the viability of this cell line, irrespective of particle size.

Conclusions

A number of features make organic conductive polymers attractive candidates for applications in which materials must interface with biological organisms. For example, many conductive polymers are synthesized routinely under biologically friendly conditions—room temperatures and aqueous media. They may also be switched chemically or electrochemically between anionic, cationic, and charge neutral states, thus providing an opportunity for triggered or selective release or uptake of small molecules. Finally, spectroscopic handles are routinely built into conductive polymers for selective chemical and biological sensing.[9]

In this paper we have shown that several conductive polymers may be synthesized as nanometer-thick coatings on gold nanoparticles. The polymers were subsequently converted into structurally rigid hollow capsules by chemically etching the particle. Loading the capsules with small molecules or larger biomolecules was accomplished by attaching the molecule to the gold particle prior to polymerization and particle removal. The particle template method thus enables the encapsulation of large molecules inside structurally rigid, mechanically stable polymeric containers. Finally, poly(pyrrole) particles with diameters ranging from 25 to 100 nm were engulfed by fibroblasts without adversely affecting normal cell viability. As we continue to develop techniques for synthesizing multilayer conductive polymer−nanoparticle composites and polymer capsules, and a deeper understanding of encapsulation and transport properties in these materials, we will begin to design multifunctional particles for intracellular diagnostics and delivery.

Acknowledgment. D.L.F. thanks the North Carolina Biotechnology Center and the NSF for support of this work, and Dr. Wallace Ambrose at the University of North Carolina for help with transmission electron microscopy. We are also grateful to Professors Barry Peters and Nina Allan for help with cell viability assays and confocal microscopy.

References and Notes

(1) (a) Templeton, A. C.; Wuelfing, W. P.; Murray, R. W. *Acc. Chem. Res.* **2000**, *33*, 27. (b) Hostetler, M. J.; Templeton, A. C.; Murray, R. W. *Langmuir* **1999**, *15*, 3782. (c) Foss, C. A., Jr.; Tierney, M. J.; Martin, C. R. *J. Phys. Chem.* **1992**, *96*, 9001. (d) Sandrock, M. L.; Pibel, C. D.; Geiger, F. M.; Foss, C. A. Jr. *J. Phys. Chem. B* **1999**, *103*, 2668. (e) Mirkin, C. A.; Letsinger, R. L.; Mucic, R. C.; Storhoff, J. J. *Nature* **1996**, *382*, 607. (f) Keating, C. D.; Feldheim, D. L. *Chem. Soc. Rev.* **1998**, *26*, 1. (g) Freeman, R. G.; Grabar, K. C.; Allison, K. J.; Bright, R. M.; Davis, J. A.; Guthrie, A. P.; Hommer, M. B.; Jackson, M. A.; Smith, P. C.; Walter, D. G.; Natan, M. J. *Science* **1995**, *267*, 1629. (h) Brust, M.; Walker, M.; Bethell, D.; Schiffrin, D. J.; Whyman, R. *J. Chem. Soc., Chem. Commun.* **1994**, 801.

(2) (a) Bateman, A. R.; Harrington, K. J.; Melcher, A. A. *Expert Opin. Inv. Drug.* **2000**, *9*, 2799. (b) Garcia-Blanco, M. A.; Puttaraju, M.; Mansfield, S. G.; Mitchell, L. G. *Gene Therapy Regulation* **2000**, *1*, 141.

(3) (a) Marinakos, S. M.; Novak, J. P.; Brousseau, L. C., III; Feldhaus, J.; House, A. B.; Feldheim, D. L. *J. Am. Chem. Soc.* **1999**, *121*, 8518. (b) Marinakos, S. M.; Shultz, D. A.; Feldheim, D. L. *Adv. Mater.* **1999**, *11*, 34. (c) Wu, M.; O'Neill, S. A.; Brousseau, L. C., III; McConnell, W.; Shultz, D. A.; Feldheim, D. L.; Linderman, R. J. *Chem. Commun.* **2000**, 775.

(4) Zhang, L.; Lu, T.; Gokel, G. W.; Kaifer, A. E. *Langmuir* **1993**, *9*, 786.

(5) Karayigitoglu, C. F.; Kommareddi, N.; Gonzalez, R. D.; John, V. T.; McPherson, G. L.; Akkara, J. A.; Kaplan, D. L. *Mater. Sci. Eng., C—Biomim2* **1995**, *2*, 165.

(6) Josephy, P.; Eling, T.; Mason, R. *J. Biol. Chem.* **1982**, *257*, 3669.

(7) Feldheim, D. L.; Krejcik, M.; Hendrickson, S. M.; Elliott, C. M. *J. Phys. Chem.* **1995**, *99* (10), 3288.

(8) Liang, W.; Martin, C. R. *Chem. Mater.* **1991**, *3*, 390.

(9) Marsella, M. J.; Carroll, P. J.; Swager, T. M. *J. Am. Chem. Soc.* **1994**, *116*, 9347.